Published in final edited form as:
J Biol Chem. 2002 May 31; 277(22): 19476–19481. doi:10.1074/jbc.M201305200.

Sphingomyelin Modulates the Transbilayer Distribution of Galactosylceramide in Phospholipid Membranes[*,S]

Peter Mattjus[‡,§], **Barbara Malewicz**[‡,§], **Jacob T. Valiyaveettil**[¶,§], **Wolfgang J. Baumann**[‡], **Robert Bittman**[¶], and **Rhoderick E. Brown**[‡,||]

‡ *University of Minnesota, Hormel Institute, Austin, Minnesota 55912*

¶ *Department of Chemistry and Biochemistry, Queens College of the City University of New York, Flushing, New York 11367–1597*

Abstract

The interrelationships among sphingolipid structure, membrane curvature, and glycosphingolipid transmembrane distribution remain poorly defined despite the emerging importance of sphingolipids in curved regions and vesicle buds of biomembranes. Here, we describe a novel approach to investigate the transmembrane distribution of galactosylceramide in phospholipid small unilamellar vesicles by ^{13}C NMR spectroscopy. Quantitation of the transbilayer distribution of [6-^{13}C] galactosylceramide (99.8% isotopic enrichment) was achieved by exposure of vesicles to the paramagnetic ion, Mn^{2+}. The data show that [6-^{13}C]galactosylceramide prefers (70%) the inner leaflet of phosphatidylcholine vesicles. Increasing the sphingomyelin content of the 1-palmitoyl-2-oleoyl-phosphatidylcholine vesicles shifted galactosylceramide from the inner to the outer leaflet. The amount of galactosylceramide localized in the inner leaflet decreased from 70% in pure 1-palmitoyl-2-oleoyl-phosphatidylcholine vesicles to only 40% in 1-palmitoyl-2-oleoyl-phosphatidylcholine/sphingomyelin (1:2) vesicles. The present study demonstrates that sphingomyelin can dramatically alter the transbilayer distribution of a monohexosylceramide, such as galactosylceramide, in 1-palmitoyl-2-oleoyl-phosphatidylcholine/sphingomyelin vesicles. The results suggest that sphingolipid-sphingolipid interactions that occur even in the absence of cholesterol play a role in controlling the transmembrane distributions of cerebrosides.

Sphingolipids participate in a number of important cellular processes that require membrane budding, fission, or vesiculation (1,2). Examples include infectious processes involving bacterial toxin and envelope virus entry into cells (3,4), exosomal antigen presentation (5), and processes related to the terminal stages of apoptosis (6). Many recent investigations, by this laboratory and others, have focused on the in-plane lateral interactions among sphingolipids, cholesterol, and other membrane lipids (7–10). As a result, significant new insights into sphingolipid organization in membranes have emerged, including the identification and characterization of sphingolipid-enriched, liquid-ordered microdomains, often referred to as rafts (11–13). With so much emphasis on lipid lateral interactions, studies of sphingolipid

[*]This work was supported by the Academy of Finland (to P. M.); NHLBI, National Institutes of Health (NIH) Grant 16660 (to R. B.), NIH Grant RR-04654 (to W. J. B.), NIGMS, NIH Grant 45928 (to R. E. B.); and by The Hormel Foundation. This investigation was presented in part at the *Phospholipid Membrane Structure Platform of the 45th Biophysical Society Annual Meeting* held in Boston, MA, February 2001 (Mattjus, P., Valiyaveettil, J. T., Malewicz, B., Bittman, R., Baumann, W. J., and Brown, R. E. (2001) *Biophys. J.* **80,** 331a).

[S]The on-line version of this article (available at http://www.jbc.org) contains Supplemental Information and Scheme 1.

||To whom correspondence should be addressed: The Hormel Inst., University of Minnesota, 801, 16th Ave. NE, Austin, MN 55912. Tel.: 507-433-8804; Fax: 507-437-9606; E-mail: rebrown@hi.umn.edu or reb@tc.umn.edu.
[§]These authors contributed equally to this study.

transmembrane distribution have been relatively few (14), and the interrelationships among sphingolipid structure, membrane curvature, and glycosphingolipid transmembrane distribution remain poorly understood (15).

Much of what is currently known about the mechanical forces affecting membrane curvature has been achieved by investigations of phosphoglyceride model membranes (16). The elastic constants associated with a fluid membrane are the bending elastic modulus and the spontaneous curvature (17,18). The bending elastic modulus is the resistance of membranes to curvature or the bending rigidity, whereas the spontaneous curvature is the inherent curvature of an unconstrained membrane section and changes with lipid structure. Because biomembranes are largely bilayers, each leaflet contributes to the overall stiffness in nonlocalized ways that arise from the different strains to which molecules in each leaflet are subjected as the bilayer bends. An outward curvature results in expansion of the outer leaflet of the bilayer along with a compression of the inner leaflet. The different strains in each leaflet produce mechanical stress gradients within the membrane. The stress gradients can significantly increase lateral diffusivity (19,20) and be a driving force for the transbilayer migration of lipid molecules between leaflets (20,21).

The altered lipid packing and stress gradients in highly curved membranes can be relieved by the generation of asymmetries in the lipid transbilayer distributions that depend on the overall molecular shape of different individual lipids (22). For instance, a well characterized lipid mass imbalance (2:1) exists in the outer and inner leaflets of phosphatidylcholine (PC)[1] small unilamellar vesicles (SUVs) as a consequence of packing the roughly cylindrically shaped PC amphiphiles into a highly curved bilayer vesicle (23,24). The resulting transbilayer lipid mass imbalance can be maintained almost indefinitely by keeping the SUVs in the liquid-crystalline phase state to minimize transient packing defects that promote slow relaxation processes (25, 26). In SUVs composed of equimolar egg phosphatidylethanolamine (PE) and egg PC, PE is enriched in the inner leaflet, whereas the PC is enriched in the outer leaflet. The smaller and less hydrated headgroup of PE imparts a cone-like molecular shape which is better suited than PC's cylindrical shape for inner leaflet localization in highly curved bilayers (27). Geometric accommodation of lipid shape also has provided a similar, logical explanation for the transbilayer distributions of lyso-PC/PC mixtures (28). However, lipid geometric shapes alone do not satisfactorily account for the transbilayer distributions observed when PC SUVs contain low mole fractions of either PE or phosphatidylglycerol (PG). In this case, disproportionately higher amounts of PE or PG are observed in the SUV outer leaflet, putatively because of generalized lattice packing effects (29,30). Together, these studies show that investigating lipid transbilayer distributions in vesicles provides an effective means to gain insights into the interrelationship between lipid structure and membrane curvature.

The present study was motivated by the need to better understand and define: 1) the transbilayer distribution of simple sphingolipids in phospholipid membranes and 2) the impact of changing vesicle composition on sphingolipid transmembrane distribution. Here, we describe a novel means to quantify the transbilayer distribution of [^{13}C]galactosylceramide (GalCer) by ^{13}C NMR. Interestingly, we find that [^{13}C]GalCer preferentially localizes to the inner leaflets of POPC SUVs. In response to increasing sphingomyelin (SPM) content, the GalCer transmembrane distribution shifts markedly toward the outer SUV leaflet even though PC and SPM have chemically identical polar headgroups. The results suggest that SPM-GalCer interactions, even in the absence of cholesterol, play an important role in controlling cerebroside transbilayer distributions.

[1]The abbreviations used are: PC, phosphatidylcholine; SUVs, small unilamellar vesicles; PE, phosphatidylethanolamine; PG, phosphatidylglycerol; GalCer, galactosylceramide; POPC, 1-palmitoyl-2-oleoyl-*sn*-glycero-3-phosphocholine; SPM, sphingomyelin; PS, phosphatidylserine.

EXPERIMENTAL PROCEDURES

Materials

POPC and egg SPM were obtained from Avanti Polar Lipids (Alabaster, AL); bovine brain GalCer without hydroxy fatty acyl chains, was from Sigma-Aldrich; and D-*erythro*-sphingosine, was from Matreya (State College, PA). [6-^{13}C]Galactose (99 atom % ^{13}C) was obtained from Omicron Biochemicals (South Bend, IN) and used to synthesize [6-^{13}C]GalCer (99.8% isotopic enrichment, Fig. 1*A*). A complete description and a scheme of the [6-^{13}C] GalCer synthesis are provided in the Supporting Information.[2] Phospholipid concentration was determined by the Bartlett method (31), and GalCer concentration was quantitated gravimetrically. Deuterated solvents ($CDCl_3$, CD_3OD, D_2O) were obtained from Cambridge Isotope Laboratories (Andover, MA).

Vesicle Preparation

SUVs were prepared by sonication using a modification of the established procedure by Huang and Thompson (25). The total amount of lipid in each preparation was kept constant (200 μmol). The lipids were dissolved in 15 ml of $CHCl_3$:CH_3OH (2:1) in a 50-ml round-bottom flask. For preparations containing GalCer, a drop of water was added to aid solubilization. A lipid film was obtained by slowly evaporating the solvents at 37 °C on a rotary evaporator, followed by freeze-drying *in vacuo* for 6 h. The lipid film was hydrated in 2 ml of D_2O, then dispersed by vortexing with intermittent warming to 37 °C, and the dispersion was sonicated under nitrogen for 30 –60 min until translucent. After removal of titanium debris by centrifugation at 50,000 × *g* for 60 min, the vesicles were used immediately for NMR analysis. Vesicle stability and vesicle impermeability to ions was ascertained by ^{31}P NMR by monitoring phospholipid chemical shifts and signal intensities as a function of time. By these criteria, all vesicles used in the present study remained stable and ion-impermeable for several days.

Localization of Phospholipids in SUVs by ^{31}P NMR

POPC and SPM were localized and quantified in the inner and outer vesicle leaflets of SUVs by ^{31}P NMR using 1 mM praseodymium (Pr^{3+}) ions as the paramagnetic shift reagent (28). Proton-decoupled ^{31}P NMR spectra were recorded at 121.42 MHz on a Varian UNITY 300 instrument (Varian Assoc., Palo Alto, CA) using a 5-mm variable temperature probe (37.0 ± 0.1 °C). Standard single-pulse experiments entailed a 90° pulse of 15 μs, an acquisition time of 1.6 s, and a pulse delay of 2 s, with the decoupler gated *on* during acquisition only. At a spectral width of 10,000 Hz, 32,000 data points were collected, whereas 1,600 and 6,400 transients were used for samples obtained in the absence and presence of Pr^{3+}, respectively. Data were then zero-filled and Fourier-transformed after applying 0.1-Hz exponential line broadening. Peak areas were digitally integrated. Spectra were referenced relative to the external standard, concentrated H_3PO_4, having a chemical shift (δ) of 0.00 ppm.

Localization of GalCer in Phospholipid SUVs by ^{13}C NMR

GalCer was localized and quantified in the inner and outer leaflets of POPC and POPC/SPM vesicles by ^{13}C NMR using 5 mM Mn^{2+}as quenching agent. Proton-decoupled ^{13}C NMR spectra of [6-^{13}C]GalCer containing SUVs were acquired at 75.423 MHz in the absolute mode at 37 °C. Standard single–pulse measurements entailed a 90° pulse of 9 μs, a pulse delay of 1 s, and an acquisition time of 1.8 s. At a spectral width of 16,500 Hz, 59,900 data points were collected, and 24,000 transients were used. Data were zero-filled and Fourier-transformed after applying 1-Hz exponential line broadening. Peak areas were digitally integrated. The integral

[2]Refs. 56–60 pertain to Supporting Information that describes the complete synthesis of [6-^{13}C]GalCer and that can be accessed on-line at the JBC web site.

of the resonance at δ 61.361 represented the total [6-^{13}C]GalCer in the vesicles (see "Results" for details). To quantify the GalCer localized in the SUV inner leaflet, 5 mM $Mn^{2+}$was added to quench the [6-^{13}C]GalCer resonance associated with the outer bilayer leaflet. The difference between the integrals of the [6-^{13}C]GalCer resonances observed at δ 61.361 in the absence (total GalCer) and in the presence (inner GalCer) of Mn^{2+}ions provided quantitation of the ion-accessible GalCer in the outer vesicle leaflet.

RESULTS

Novel Approach to Measure Glycolipid Transbilayer Distribution in Phospholipid Vesicles by ^{13}C NMR

Phospholipid transbilayer distribution between the inner and outer leaflets of vesicles can be accurately determined by ^{31}P NMR (32–34). However, this approach is not suitable for monitoring the transbilayer distribution of glycosphingolipids because of the lack of phosphate in the headgroup of these lipids. Thus, the localization of the sugar headgroups of glycosphingolipids incorporated into vesicles was analyzed by ^{13}C NMR spectroscopy.

A comparison of ^{13}C NMR spectra of phospholipids (35) and of bovine brain GalCer in solution ($CDCl_3$:CD_3OD:D_2O; 50:50:15, v/v/v; Fig. 1*B*), indicated that two signature resonances derived from C-6 and C-1 of galactose (δ 61.445 and 104.083, respectively) did not overlap with any of the phospholipid resonances and thus might be used for quantitative analysis. However, preliminary experiments with vesicles composed of PC, SPM, and GalCer (40:40:20 mol %) indicated that only the 61.361-ppm resonance derived from C-6 of galactose could be clearly detected, whereas the C-1 resonance was broadened almost beyond recognition (data not shown). This finding is consistent with C-1 being more motionally restricted by virtue of being part of the pyranose ring and buried in the membrane interfacial region. In contrast, the C-6 carbon is not part of the rigid ring system, can rotate more freely, and projects farther into the aqueous phase (36). Thus, the ^{13}C NMR resonance of the galactose C-6 carbon was deemed best suited for quantifying the transbilayer distribution of GalCer in vesicles.

Attempts to shift the GalCer C-6 resonance (δ 61.361) using paramagnetic shift reagents ($Pr^{3+}$and Yb^{3+}) yielded unsatisfactory results, leading us to adopt an alternate approach to quantify GalCer in the inner and outer vesicle leaflets of SUVs. Our approach was based on using Mn^{2+}ions as a bilayer-impermeant relaxing reagent to measure the distribution of cholesterol in the inner and outer leaflets of lipid vesicles.[3] A similar strategy has previously been used to compare the accessibility of cholesterol in the outer leaflet of ester- and ether-linked phospholipid SUVs (39). Titration experiments revealed that 5 mM $Mn^{2+}$was optimal for efficiently quenching the resonance at 61.361 ppm derived from GalCer in the vesicle outer leaflet without affecting the resonances of the inner leaflet. Because of the relatively low signal intensity of the C-6 resonance of GalCer compared with the phospholipid resonances in SUVs, natural abundance ^{13}C NMR required that the vesicles contain a relatively high content of GalCer (>20 mol %) to achieve adequate signal-to-noise ratios to quantify the transbilayer distribution of GalCer. To monitor GalCer transbilayer distribution over a wide range of mole fractions, including those typical of biological membranes, isotopic enrichment at the C-6 position of galactose was deemed the best strategy to assure acceptable sensitivity. Thus, we synthesized [6-^{13}C]GalCer as described in detail in the Supplemental Information and outlined in Scheme 1. The resulting preparation was 99.8% isotopically enriched and increased the intensity of the GalCer C-6 resonance almost 100-fold (Fig. 1*A*).

[3]B. Malewicz and W. J. Baumann, unpublished data.

Transmembrane Distribution of GalCer in POPC Vesicles

To determine GalCer distribution in phospholipid vesicles, POPC SUVs containing 1 mol % [6-^{13}C]GalCer were prepared and analyzed by ^{13}C NMR at 37 °C. Fig. 2 shows that the C-6 resonance of galactose was well separated from POPC resonances and that its signal-to-noise ratio (~20:1) was well suited for quantitative analysis. Fig. 3 (*left panel*) shows the 50 –75-ppm region of the ^{13}C NMR spectrum of the POPC vesicles containing 1 mol % [6-^{13}C]GalCer before and after addition of 5 mM Mn^{2+}. It is noteworthy that GalCer strongly preferred the inner leaflet (Fig. 3, *right panel*), with 70% of the GalCer molecules being inaccessible to Mn^{2+}ions (Table I). The same high preference of GalCer for the inner leaflet of POPC SUVs also was observed when the GalCer content was increased to 2 mol% (Fig. 3, *right panel*; Table I).

To determine the transbilayer distribution of POPC in SUVs containing 1 or 2 mol % GalCer, ^{31}P NMR measurements were performed in the presence and absence of Pr^{3+}(see “Experimental Procedures”). The outer-to-inner leaflet phosphorus ratios were 1.94 and 1.92, respectively, and were similar to the 1.90 ratio of pure POPC SUVs (Table I).

SPM Alters the Transmembrane Distribution of GalCer

To investigate the effect of increasing SPM on the transbilayer distribution of GalCer, SUVs with a constant amount of [6-^{13}C]GalCer and varying amounts of POPC and SPM (*e.g.* 2:1, 1:1, or 1:2) were prepared. The transbilayer distributions of [6-^{13}C]GalCer and of each phospholipid were then assessed by ^{13}C and ^{31}P NMR spectroscopy, respectively. Fig. 4 (*left panel*) shows the ^{31}P NMR spectra of vesicles composed of equimolar POPC and egg SPM containing 1 mol % GalCer. As the top spectrum illustrates, the ^{31}P resonances of POPC (−0.900 ppm) and SPM (−0.246 ppm) were partially resolved from each other in the absence of Pr^{3+}, indicating differing local environments for their phosphocholine headgroup moieties. Addition of Pr^{3+}caused the POPC and SPM resonances of the SUV outer leaflet to shift downfield, resulting in the four distinct resonance peaks shown in the lower spectrum of Fig. 4. By comparison with SUVs containing different amounts of SPM and POPC (*e.g.* 1:2 and 2:1), the SPM and POPC resonances were assigned to the inner (−0.246 and −0.900 ppm, respectively) and outer (7.596 and 5.203 ppm, respectively) leaflets. The peak assignments agree well with earlier reports (35–38). The larger Pr^{3+}-induced downfield shift of outer leaflet SPM (compared with PC) and the distinct ^{31}P resonances of SPM and POPC in the absence of lanthanide ions were consistent with earlier findings (32,38,40). Quantitative assessment indicated that the content of phospholipid (both POPC and SPM) in the outer leaflet of SUVs far exceeded that in the inner leaflet, consistent with the known mass distribution of PC in SUVs of ~25-nm diameter (Fig. 4). However, small but reproducible differences in the transbilayer distributions of POPC and SPM could be distinguished (Table I). SPM showed a slightly greater preference for the outer leaflet at the expense of POPC and this tendency became more pronounced as the SPM mole fraction increased. It is also noteworthy that the overall outside-to-inside ^{31}P integrated signal ratios of the SPM/POPC vesicles remained very close to the 2:1 ratio expected for SUVs at all SPM compositions, consistent with the vesicles having average diameters of ~25 nm (23,25,26). Previous studies have indicated that sonication of SPM results in formation of unilamellar vesicles similar in size to those generated by sonication of PCs (40).

Having established the transbilayer distribution of SPM and POPC when mixed in SUVs, we next determined the effect of SPM on the transbilayer distribution of 1 mol % [6-^{13}C]GalCer by ^{13}C NMR (Fig. 5). We found that increasing the SPM content in POPC SUVs shifted GalCer from the inner to the outer leaflet. The amount of GalCer localized to the inner leaflet decreased from 70% in pure POPC vesicles to only 40% in POPC/SPM (1:2) vesicles. We believe that

this represents the first evidence showing that SPM can dramatically alter the transbilayer distribution of a simple monohexosylceramide, such as GalCer, in phospholipid vesicles.

DISCUSSION

We have quantified the transbilayer distribution of GalCer in phospholipid vesicles by ^{13}C NMR spectroscopy. When used in combination with ^{31}P NMR approaches that monitor phospholipid transbilayer distribution, the strategy provides novel insights into the effect of changing SPM content on the transbilayer distribution of simple glycosphingolipids. The results reveal two notable findings. First, at low mole fractions, GalCer strongly prefers the *inner* leaflet of POPC SUVs. Second, increasing the SPM content of the POPC SUVs shifts the transbilayer distribution of GalCer toward the outer leaflet. Ramifications of these observations are discussed below.

In POPC SUVs containing low mole fractions of GalCer (1 or 2 mol %), 70% of the glycolipid is localized in the inner leaflet. This corresponds to a doubling of the GalCer inner membrane concentration with respect to POPC, which is 34% localized in the inner leaflet (Table I). The mass distribution of PC in SUVs (1:2 inner leaflet-to-outer leaflet) is well established (7–9). What is remarkable about the transmembrane distribution of GalCer is its strong preference for the inner leaflet when present at 1 or 2 mol % in POPC SUVs. Earlier studies of PE and PG (see Introduction) revealed just the opposite behavior in that these lipids strongly preferred the outer leaflet of PC SUVs (29,30). Only when present at 10 mol % (or more) in PC SUVs did PE and PG assume transmembrane distributions that can be rationalized by the structural parameters associated with their overall shape, charge, and hydration (22,29,30). The preferential localization of low mole fractions of PE and PG to the outer leaflet of PC SUVs has been explained as a general lattice response linked to the “looser” molecular packing of the outer leaflet of PC SUVs (30). Our results clearly show that GalCer does not conform to the PE/PG transmembrane localizations in fluid PC bilayers previously reported for highly curved phosphoglyceride vesicles. This may be a consequence of GalCer having a completely uncharged and moderately hydrated polar headgroup compared with the zwitterionic or ionic headgroups of phosphoglycerides (36,41).

The second major finding of this study is that increasing the SPM content of POPC SUVs dramatically shifts the transbilayer distribution of GalCer toward the outer leaflets. This shift occurs even though SPM and POPC have chemically identical phosphocholine headgroups. Not surprisingly, our ^{31}P NMR measurements in the presence and absence of the paramagnetic shift ion, Pr^{3+}, show that SPM and POPC localize quite similarly in SUVs with SPM showing only a slight preference for the outer leaflet (38,40). However, the impact of increasing SPM content on GalCer transmembrane distribution is clear and dramatic (Table I). It is likely that the remarkable shift in the transbilayer localization of GalCer toward the outer leaflets of SPM/POPC SUVs reflects changes in the in-plane interactions that occur between GalCer and SPM relative to those that occur between GalCer and POPC in highly curved vesicles. The structural features of GalCer, SPM, and POPC likely to play a role in this behavior are the following. First, consider the lipid hydrocarbon region. POPC has the naturally prevalent PC motif consisting of *sn*-1 chain saturation and *sn*-2 chain unsaturation. Both egg SPM and [6-^{13}C] GalCer have the naturally prevalent sphingolipid motif consisting of sphingosine and a saturated acyl chain. Compared with POPC’s oleoyl chains, the mostly palmitoyl acyl chains (~85%) of egg SPM would be expected to pack better with the palmitoyl chains of [6-^{13}C] GalCer. With regard to the polar headgroup region, one might mistakenly assume no difference among PC and SPM because of the chemical identity of their phosphocholine head-groups. However, it is clear that, when PC and SPM are mixed together in SUVs, the ^{31}P NMR resonances of these lipids display different chemical shifts, indicating that the local environments near their respective phosphate groups are not identical. One explanation may

be that SPM, but not PC, forms intramolecular hydrogen bonds involving the hydroxyl group at carbon 3 of the sphingoid base and either the bridge oxygen or ester oxygen of phosphate (40,42–44). This capability may contribute to the metastable behavior and different structural conformations known to occur in SPMs (Refs. 43–46 and references therein). In addition, the ceramide region of SPM and GalCer contain amide-linked acyl chains, which are thought to participate in intermolecular hydrogen bonding lattices via bridging water molecules, as well as 4,5-trans double bonds that further modulate intermolecular interactions (10,42). The combined differences in the headgroup and interfacial regions of SPMs and PCs appear likely to affect their interactions with GalCer. Altogether, our results emphasize that subtle structural and conformational changes to the interfacial zone of bilayer matrix lipids, such as PC and SPM, can significantly affect the transbilayer distribution of simple sphingolipids, such as cerebroside, in curved membranes.

Physiological Relevance and Implications

Lipid transmembrane asymmetry is of fundamental importance to the health of cells, and a loss of this asymmetry has severe detrimental effects. During late apoptotic events as well as under many other pathological conditions such as diabetes, malaria, and sickle cell disease, a loss of phosphatidylserine (PS) asymmetry occurs (47). A defect in the aminophospholipid translocase or activation of the phospholipid scramblase causes abnormal exposure of PS on the exoplasmic leaflet from its normal cytoplasmic orientation (48–50). PS externalization during the lipid scrambling process has recently been linked to the inward translocation of external SPM (6). This “flopped” SPM pool is hydrolyzed by cytosolic sphingomyelinase to ceramide as part of the execution phase of apoptosis. SPM depletion from the plasma membrane leads to a redistribution of cholesterol to intracellular sites and/or the efflux of cholesterol to external acceptors such as serum lipoproteins and cyclodextrins (51,52). An important consequence of SPM transmembrane migration and associated ceramide generation is a triggering of membrane destabilization and an increase in membrane fission processes involving membrane blebbing and vesicle shedding. Other striking examples implicating sphingolipid transmembrane distributions in the triggering of membrane vesiculation in cell and model membranes also have been reported (1,53).

Gaining insights into the effects of high curvature on membranes is an area of increasing interest in cell biology because of the importance of membrane fission events in generating transport vesicles (54). The ability of endophilin, a presynaptically enriched protein that binds the GTPase dynamin and synptojanin, to generate very highly curved membrane tubules underscores the potential importance of tubulovesiculation processes to membrane trafficking events in the cell (55). Investigations of sphingolipid transbilayer distributions in curved membranes of defined composition, such as those reported here, are likely to provide a valuable foundation for a better understanding of cellular processes initiated by or utilizing curved membrane regions where sphingolipids are important.

Supplementary Material

Refer to Web version on PubMed Central for supplementary material.

References

1. Zha X, Pierini M, Leopold PL, Skiba PJ, Tabas I, Maxfield FR. J Cell Biol 1998;140:39–47. [PubMed: 9425152]
2. Smart EJ, Graf GA, McNiven MA, Sessa WC, Engelman JA, Scherer PE, Okamoto T, Lisanti MP. Mol Cell Biol 1999;19:7289–7304. [PubMed: 10523618]
3. Lingwood CA, Boyd B, Nutikka A. Methods Enzymol 2000;312:459–473. [PubMed: 11070894]

4. Hug P, Lin HM, Korte T, Xiao XD, Dimitrov DS, Wang JM, Puri A, Blumenthal R. J Virol 2000;7:6377–6385. [PubMed: 10864648]
5. Denzer K, Kleijmeer MJ, Heijnen HFG, Stoorvogel W, Geuze HJ. J Cell Sci 2000;113:3365–3374. [PubMed: 10984428]
6. Tepper AD, Ruurs P, Wiedmer T, Sims PJ, Borst J, van Blitterswijk WJ. J Cell Biol 2000;150:155–164. [PubMed: 10893264]
7. Li XM, Momsen MM, Brockman HL, Brown RE. Biochemistry 2001;40:5954–5963. [PubMed: 11352730]
8. Dietrich C, Bagatolli LA, Volovyk ZN, Thompson NL, Levi M, Jacobson K, Gratton E. Biophys J 2001;80:1417–1428. [PubMed: 11222302]
9. Brown RE. J Cell Sci 1998;111:1–9. [PubMed: 9394007]
10. Masserini M, Ravasi D. Biochim Biophys Acta 2001;1532:149–161. [PubMed: 11470236]
11. Simons K, Ikonen E. Nature 1997;387:569–572. [PubMed: 9177342]
12. Brown DA, London E. J Biol Chem 2000;275:17221–17224. [PubMed: 10770957]
13. van der Goot FG, Harder T. Semin Immunol 2001;13:89–97. [PubMed: 11308292]
14. Sillence DJ, Raggers RJ, van Meer G. Methods Enzymol 2000;312:562–579. [PubMed: 11070902]
15. Maggio B. Prog Biophys Mol Biol 1994;62:55–117. [PubMed: 8085016]
16. Sackmann, E. Structure and Dynamics of Membranes. Lipowsky, R.; Sackmann, E., editors. 1A. Elsevier Science Publishing Co., Inc.; New York: 1995. p. 213-304.
17. Evans E, Needham D. J Phys Chem 1987;91:4219–4228.
18. Helfrich W. Z Naturforsch 1973;28C:693–703.
19. Evans EA, Yeung A. Chem Phys Lipids 1994;73:39–56.
20. Raphael RM, Waugh RE. Biophys J 1996;71:1374–1388. [PubMed: 8874013]
21. Svetina S, Zeks B, Waugh RE, Raphael RM. Eur Biophys J Biophys Lett 1998;27:197–209.
22. Israelachvili JN, Mitchell DJ, Ninham BW. Biochim Biophys Acta 1977;470:185–201. [PubMed: 911827]
23. Yeagle PL, Hutton WC, Martin RB, Sears BJ, Huang C. J Biol Chem 1976;251:2110–2112. [PubMed: 1270423]
24. Huang C, Mason JT. Proc Natl Acad Sci U S A 1978;75:308–310. [PubMed: 272647]
25. Huang C, Thompson TE. Methods Enzymol 1974;32:485–489. [PubMed: 4475349]
26. Lichtenberg D, Barenholz Y. Methods Biochem Anal 1988;33:337–462. [PubMed: 3282152]
27. Litman BJ. Biochemistry 1974;13:2844–2848. [PubMed: 4407872]
28. Kumar VV, Baumann WJ. Biochem Biophys Res Commun 1986;139:25–30. [PubMed: 3767957]
29. Lentz BR, Litman BJ. Biochemistry 1978;17:5537–5543. [PubMed: 728414]
30. Lentz BR, Alford DR, Dombrose FA. Biochemistry 1980;19:2555–2559. [PubMed: 7190434]
31. Bartlett GR. J Biol Chem 1959;234:466–468. [PubMed: 13641241]
32. Berden JA, Barker RW, Radda GK. Biochim Biophys Acta 1975;375:186–208. [PubMed: 235977]
33. Kumar VV, Malewicz B, Baumann WJ. Biophys J 1989;55:789–792. [PubMed: 2720071]
34. Kumar VV, Anderson WH, Thompson EW, Malewicz B, Baumann WJ. Biochemistry 1988;27:393–398. [PubMed: 3349040]
35. Murari R, Abd El-Rahman MMA, Wedmid Y, Parthasarathy S, Baumann WJ. J Org Chem 1982;47:2158–2163.
36. Bruzik KS, Nyholm PG. Biochemistry 1997;36:566–575. [PubMed: 9012672]
37. Tkaczuk P, Thornton ER. Biochem Biophys Res Commun 1979;91:1415–1422. [PubMed: 575043]
38. Castellino FJ. Arch Biochem Biophys 1978;189:465–470. [PubMed: 568454]
39. Bittman R, Clejan S, Lund-Katz S, Phillips MC. Biochim Biophys Acta 1984;772:117–126. [PubMed: 6722139]
40. Schmidt CF, Barenholz Y, Thompson TE. Biochemistry 1977;16:2649–2656. [PubMed: 889781]
41. Ruocco MJ, Shipley GG. Biochim Biophys Acta 1983;735:305–308. [PubMed: 6626552]

42. Talbott CM, Vorobyov I, Borchman D, Taylor KG, DuPre DB, Yappert MC. Biochim Biophys Acta 2000;1467:326–337. [PubMed: 11030591]
43. Bruzik KS. Biochim Biophys Acta 1988;939:315–326. [PubMed: 3355820]
44. Bruzik KS, Sobon B, Salamonczyk GM. Biochemistry 1990;29:4017–4021. [PubMed: 2354174]
45. Maulik PR, Shipley GG. Biochemistry 1996;35:8025–8034. [PubMed: 8672507]
46. Maulik PR, Shipley GG. Biophys J 1996;70:2256–2265. [PubMed: 9172749]
47. Closse C, Dachary-Prigent J, Boisseau MR. Br J Haematol 1999;107:300–302. [PubMed: 10583215]
48. Bratton DL, Fadok VA, Richter DA, Kailey JM, Guthrie LA, Henson PM. J Biol Chem 1997;272:26159–26165. [PubMed: 9334182]
49. Frasch SC, Henson PM, Kailey JM, Richter DA, Janes MS, Fadok VA, Bratton DL. J Biol Chem 2000;275:23065–23073. [PubMed: 10770950]
50. Bevers EM, Comfurius P, Dekkers DWC, Zwaal RFA. Biochim Biophys Acta 1999;1439:317–330. [PubMed: 10446420]
51. Ohvo H, Olsio C, Slotte JP. Biochim Biophys Acta 1997;1349:131–141. [PubMed: 9421186]
52. Rothblat GH, de la Llera-Moya M, Atger V, Kellner-Weibel G, Williams DL, Phillips MC. J Lipid Res 1999;40:781–796. [PubMed: 10224147]
53. Holopainen JM, Angelova MI, Kinnunen PKJ. Biophys J 2000;78:830–838. [PubMed: 10653795]
54. Huttner WB, Zimmerberg J. Curr Opin Cell Biol 2001;13:478–484. [PubMed: 11454455]
55. Farsad K, Ringstad N, Takie K, Floyd SR, Rose K, De Camilli P. J Cell Biol 2001;155:193–200. [PubMed: 11604418]
56. Fiandor J, Garcia-Lopez MT, de las Heras FG, Mendez-Castrillon PP. Synthesis 1985;12:1121–1123.
57. Wegmann B, Schmidt RR. J Carbohydr Chem 1987;6:357–375.
58. Vasella A, Witzig C, Martin-Lomas M. Helv Chim Acta 1991;74:2073–2077.
59. Rui Y, Thompson DH. J Org Chem 1994;59:5758–5762.
60. Gololobov YG, Zhmurova IN, Kasukhin LF. Tetrahedron 1981;37:437–472.

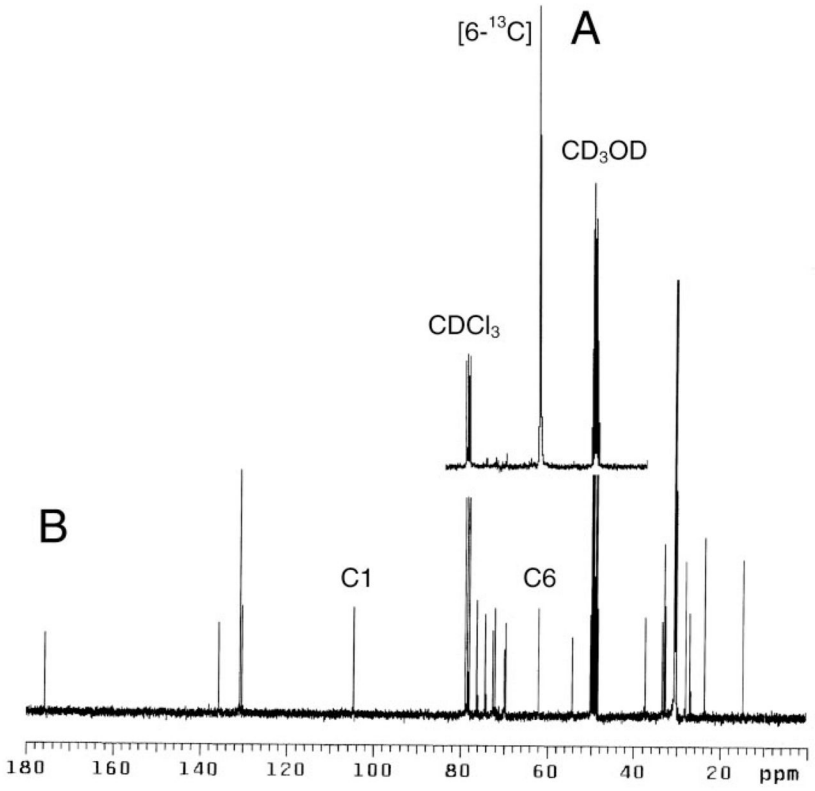

Fig. 1. Solution spectra of GalCer

A, ^{13}C NMR of [6-^{13}C]GalCer. *B*, natural abundance ^{13}C NMR of bovine brain GalCer (without hydroxy fatty acyl chains). Both spectra were acquired in $CDCl_3$: CD_3OD:D_2O (50:50:15 v/v/v). *C1* and *C6* indicate resonances of galactose.

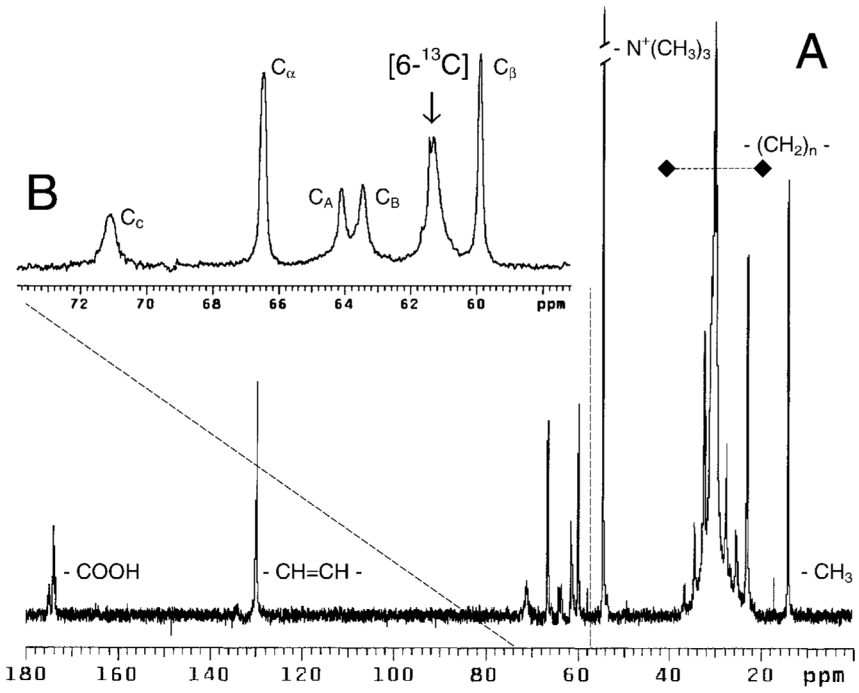

Fig. 2. ^{13}C NMR spectrum of [6-^{13}C]-GalCer-POPC vesicles

Inset B shows an expanded δ region between 50 and 73 ppm. C_A, C_B, and C_C indicate the resonances of the glycerol carbons, and $C\alpha$ and $C\beta$ indicate the phosphocholine head-group resonances. The POPC vesicles contained 1 mol % [6-^{13}C]GalCer.

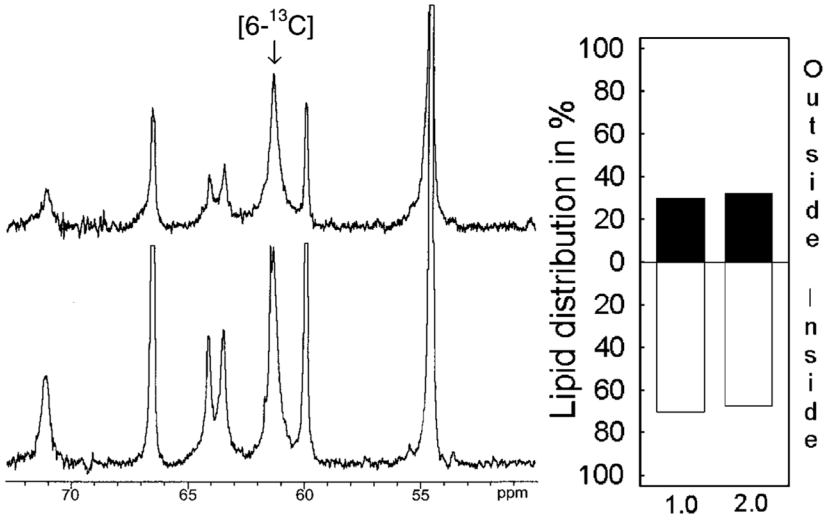

Fig. 3. Transbilayer distribution of GalCer in POPC vesicles determined by ^{13}C NMR

Left panel, ^{13}C NMR spectra (55–75-ppm region) of POPC vesicles containing 1 mol % [6-^{13}C]GalCer, acquired in the absence (*lower spectrum*), and in the presence of 5 mM Mn^{2+}(*upper spectrum*). *Right panel*, transbilayer distribution of GalCer in POPC vesicles containing either 1 or 2 mol % [6-^{13}C]GalCer.

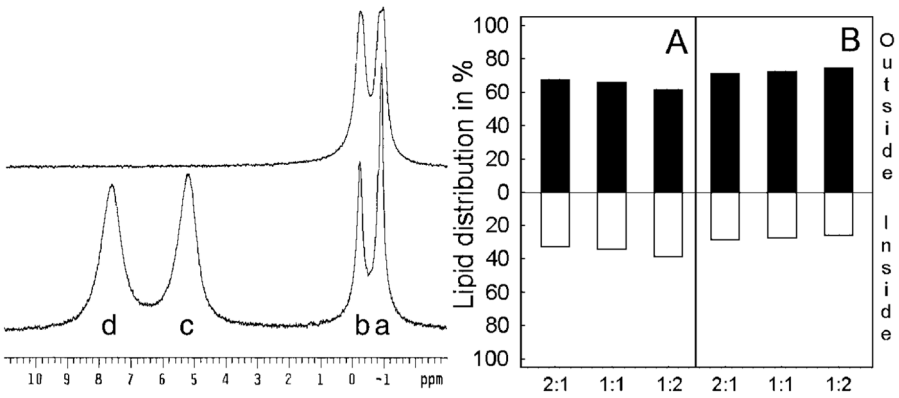

Fig. 4. Transbilayer distribution of POPC and SPM determined by ^{31}P NMR

Left panel, ^{31}P NMR spectra of vesicles comprised of equimolar POPC and SPM and containing 1 mol % [6-^{13}C]GalCer, acquired in the absence (*upper spectrum*), and in the presence of 1 mM Pr^{3+} (*lower spectrum*). The *lower spectrum* shows well resolved resonances derived from POPC (*a*) and SPM (*b*) of the inner leaflet and from POPC (*c*) and SPM (*d*) of the outer leaflet. *Right panel*, transbilayer distribution of POPC (*A*) and SPM (*B*) measured from ^{31}P NMR data for vesicles comprised of POPC/SPM at the molar ratios of 2:1, 1:1, and 1:2 and containing 1 mol % [6-^{13}C]GalCer.

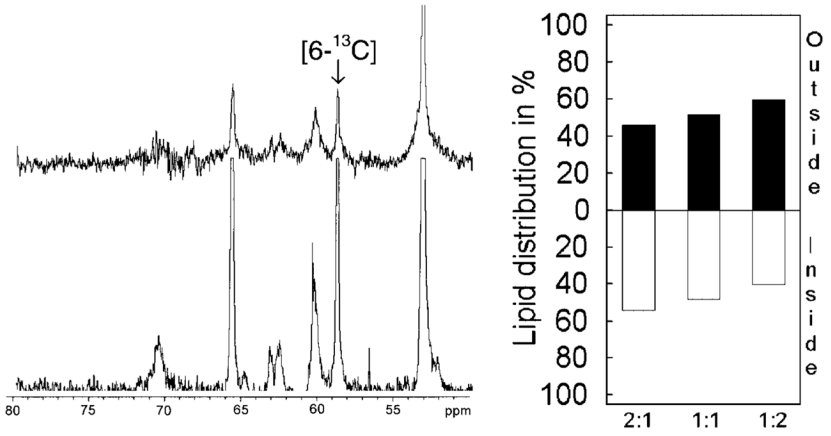

Fig. 5. The effect of SPM on the transbilayer distribution of GalCer determined by ^{13}C NMR

Left panel, ^{13}C NMR spectra (50 –80-ppm region) of vesicles comprised of equimolar POPC and SPM and containing 1 mol % [6-^{13}C]GalCer, acquired in the absence (*lower spectrum*) and in the presence of 5 mM Mn^{2+}(*upper spectrum*). *Right panel*, transbilayer distribution of GalCer in vesicles composed of POPC/SPM at the molar ratios of 2:1, 1:1, and 1:2 and containing 1 mol % [6-^{13}C]GalCer.

Table I

GalCer, SPM, and POPC transbilayer distributions in SUVs

The inner and outer leaflet compositions of the vesicles were calculated from NMR data acquired as described under “Experimental Procedures.” Units are expressed as mol %.

Lipid	PC (100)	PC:GalCer (99:1)	PC:GalCer (98:2)	PC:SPM:GalCer (66:33:1)	PC:SPM:GalCer (49.5:49.5:1)	PC:SPM:GalCer (33:66:1)
$POPC_{outside}$	65.5	66.0	65.7	67.4	65.8	61.5
$POPC_{inside}$	34.5	34.0	34.4	32.6	34.2	38.5
$SPM_{outside}$				71.3	72.4	74.2
SPM_{inside}				28.7	27.6	25.8
$GalCer_{outside}$		29.9	32.5	45.9	51.6	59.7
$GalCer_{inside}$		70.1	67.5	54.1	48.4	40.3